



Catalytic performance in selective hydrogenation of citral of bimetallic Pt–Sn catalysts supported on MgAl₂O₄ and γ-Al₂O₃

Patricia D. Zgolicz*, Virginia I. Rodríguez, Irene M.J. Vilella, Sergio R. de Miguel, Osvaldo A. Scelza

Instituto de Investigaciones en Catálisis y Petroquímica (INCAPE), Facultad de Ingeniería Química, Universidad Nacional del Litoral – CONICET, Santiago del Estero 2654, 3000 Santa Fe, Argentina

ARTICLE INFO

Article history:

Received 23 July 2010

Received in revised form 3 November 2010

Accepted 5 November 2010

Available online 16 November 2010

Keywords:

Citral selective hydrogenation

Supported PtSn catalysts

MgAl₂O₄

γ-Al₂O₃

Characterization of the metallic phase

ABSTRACT

The liquid phase citral hydrogenation, using Pt and PtSn catalysts supported on MgAl₂O₄ and γ-Al₂O₃, was studied in a stirred reactor at 70 °C and atmospheric pressure. It was found that the addition of Sn to the Pt catalysts increases the selectivity to double unsaturated alcohols for both catalyst series. Besides, monometallic catalysts hydrogenate the α,β-unsaturation with a high selectivity in absence of cyclization secondary products. The performance of these catalysts in the citral hydrogenation was related with the characteristics of the metallic phase. Results from test reactions – cyclohexane dehydrogenation (CHD) and cyclopentane hydrogenolysis (CPH) – H₂ chemisorption, 2-propanol dehydration, temperature programmed reduction (TPR) and X-ray photoelectron spectroscopy (XPS), were used to explain the influence of the support and the Sn loading and postulate the models of the catalytic metallic surface. Results indicated that, a fraction of ionic Sn would be deposited near Pt, thus increasing the polarization of the carbonyl group, and a fraction of metallic Sn could form Pt–Sn alloy phases that would hinder the hydrogenation of the olefinic bonds and would be active to the hydrogenation of the carbonyl group. Both effects contribute to a higher selectivity to unsaturated alcohols in bimetallic PtSn/Al₂O₃ catalysts than PtSn/MgAl₂O₄ ones, which display a low alloy formation.

© 2010 Elsevier B.V. All rights reserved.

1. Introduction

The production of α,β-unsaturated alcohols is a very interesting process since it leads to the obtention of very important intermediaries of organic synthesis used in the manufacture of allyl ethers and allyl esters, and final products for Fine Chemistry used in perfumery and pharmacy [1–4]. The selective hydrogenation of unsaturated α,β aldehydes to produce the corresponding unsaturated alcohols is a difficult reaction due to the double olefinic bonds are preferably hydrogenated, both by thermodynamic and kinetic reasons. The use of monometallic catalysts based on Pt, Pd, Ru or Ni supported on non reducible oxides [5–8] leads mainly to the formation of saturated aldehydes. In consequence a modification of the metallic phase is necessary to obtain the desirable products. In order to increase the selectivity of monometallic catalysts in the hydrogenation of carbonyl group, several studies [5,9–14] have been carried out to study the effect of the support, promoter addition, metallic particle size and solvents used in the reaction. In particular, it was found that the addition of Sn, Ge, Fe, and Ga to Pt catalysts [10,15,16] can strongly modify the catalytic properties of the metal active by the presence of geometric and/or electronic effects, which would

be responsible for the increment of the selectivity to unsaturated alcohols. In this sense, the behaviour of the PtSn systems has been explained as caused by the promotion effect of oxidized species of Sn (placed near to Pt atoms) that promote the carbonyl hydrogenation [17–22]. In this case the interaction of the oxidized Sn species with the oxygen of the carbonyl group could weaken the C=O bond and hence enhance the carbonyl hydrogenation rate. However, the presence of metallic Sn was found by XPS, XRD and TEM in several studies on selective hydrogenation of unsaturated α,β aldehydes [17,20,23–30] and it was considered as an important parameter of the catalytic activity in PtSn catalysts. The metallic Sn could be forming aggregates which produce a geometric effect on the metallic phase [21,25,29]. Besides, this metallic Sn can be alloyed with Pt, thus avoiding the hydrogenation of the olefinic double bond or showing activity to the hydrogenation of the carbonyl group, and in this way it would increase the selectivity to unsaturated alcohols [17,23,26,28,30–32].

Even though there are several papers on the catalytic behaviour of mono and bimetallic catalysts based on Pt supported on Al₂O₃ [5,23,29,30,33–43] in selective hydrogenation of α,β-unsaturated aldehydes, there is practically no information on mono and bimetallic catalysts based on Pt supported on spinels [44]. Besides, it must be noted that none of these papers report the selective hydrogenation of citral (3,7-dimethyl-2,6-octadienal) to unsaturated alcohols.

* Corresponding author. Tel.: +54 342 4555279.

E-mail address: pzgolicz@fiq.unl.edu.ar (P.D. Zgolicz).

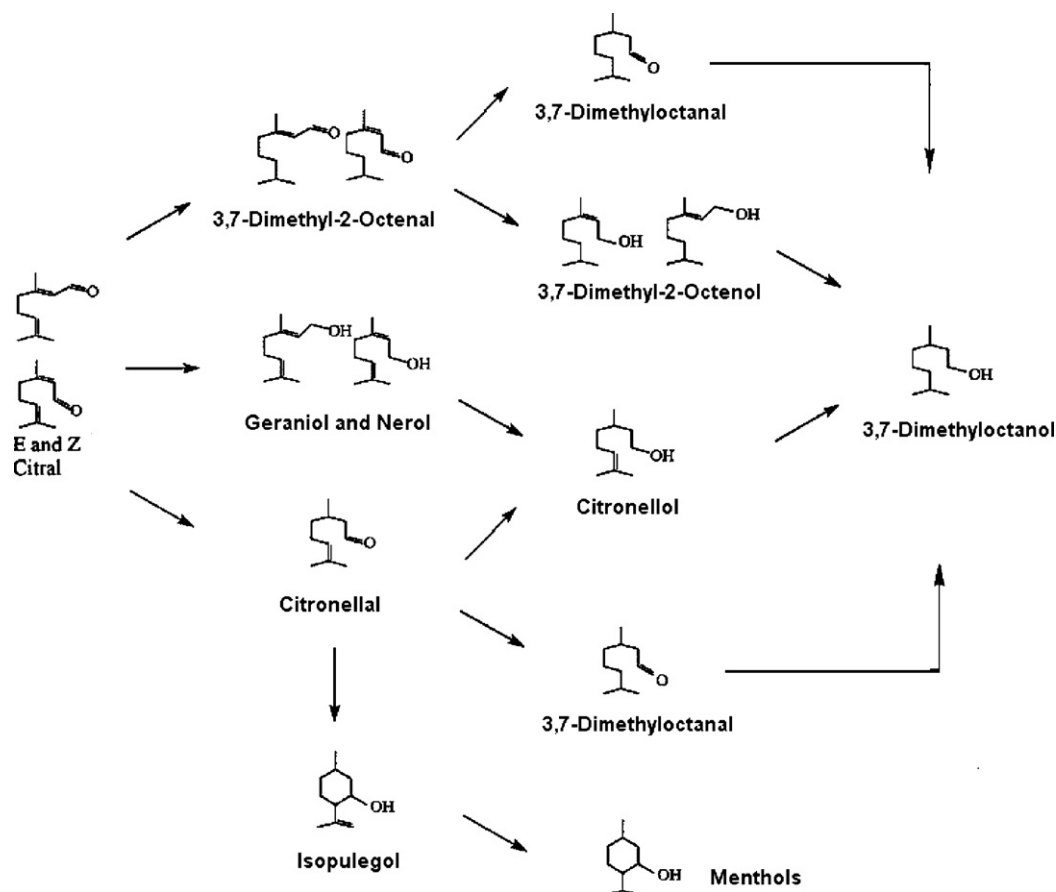


Fig. 1. Main reaction routes in citral hydrogenation.

The objective of this paper is to study the catalytic behaviour in the citral hydrogenation of Pt and PtSn catalysts supported on MgAl_2O_4 and Al_2O_3 . In this sense the effect of the Sn amount added to a given Pt loading for both supports was investigated. The bimetallic catalysts were prepared by successive impregnation of the corresponding support. The catalysts were submitted to different characterization techniques: test reactions of the metallic phase (cyclohexane dehydrogenation and cyclopentane hydrogenolysis), H_2 chemisorption, temperature programmed reduction (TPR) and X-ray photoelectron spectroscopy (XPS), and the support acidity was examined by 2-propanol dehydration. For this study the citral hydrogenation was selected, because citral is an abundant raw material from the lemongrass oil. Besides, citral is a very interesting molecule model since it has three different unsaturated bonds: a carbonyl group, a double $\text{C}=\text{C}$ bond conjugated with the carbonyl group and one isolated $-\text{C}=\text{C}-$ bond. It also exists as cis and trans isomers and it can also be cyclized. Fig. 1 shows the main products which can be obtained by hydrogenation and cyclization.

2. Experimental

2.1. Preparation of the catalysts

Two supports were used: (i) MgAl_2O_4 (obtained in the laboratory, $S_{\text{BET}} = 108 \text{ m}^2 \text{ g}^{-1}$) with a spinel structure and equilibrium $\text{pH} = 8.6$, and (ii) commercial $\gamma\text{-Al}_2\text{O}_3$ (CK 300 from Cyanamid Ketjen, $S_{\text{BET}} = 180 \text{ m}^2 \text{ g}^{-1}$) previously calcined at 650°C . The first support was prepared by using the co-precipitation method [45] from solutions of $\text{Mg}(\text{NO}_3)_2 \cdot 6\text{H}_2\text{O}$ (Merck, purity 99%), $\text{Al}(\text{NO}_3)_3 \cdot 9\text{H}_2\text{O}$ (Merck, purity 98.5%) and ammonia solution (Merck, 28%, analytical grade). 0.5 M solutions of Al and Mg

nitrate with a Al/Mg molar ratio = 2 were used for the preparation of the precursor by slow addition of aqueous solution of ammonia under stirring, until reaching $\text{pH} = 11$ at 40°C . After its formation, the precursor gel was aged for 1 h at room temperature and then filtered. The gel was washed with an excess of distilled water (volume ratio water/gel = 4) under stirring and filtered again. Additionally, the gel was washed in the same filter paper with distilled water. Then it was dried at 120°C overnight, and finally calcined at 800°C for 4 h. Monometallic Pt catalysts (5 wt%) were prepared by impregnation (25°C for 6 h) of the corresponding support with an aqueous solution of H_2PtCl_6 (12.6 g L^{-1}), by using an impregnation volume/mass of support ratio = 4 mL g^{-1} . After impregnation the samples were dried at 120°C overnight and then calcined at 500°C for 3 h. The bimetallic catalysts of Pt(5 wt%)Sn(1, 2, 3 or 4 wt%)/ MgAl_2O_4 and Pt(5 wt%)Sn(1, 2 or 3 wt%)/ Al_2O_3 were prepared by successive impregnation of the monometallic ones. Thus, the precursor of the monometallic catalyst was impregnated for 6 h at room temperature with a hydrochloric solution of SnCl_2 by using a Sn concentration such as to obtain 1, 2, 3 or 4 wt% Sn when the support was MgAl_2O_4 and 1, 2 or 3 wt% when the support was Al_2O_3 . It was used a volume of impregnation/mass of support ratio of 1.4 mL g^{-1} for catalysts with 1 and 2% of Sn. The impregnating volume/support weight ratios were 2 and 3 mL g^{-1} for 3 and 4 wt% Sn loading, respectively. Finally the samples were dried at 120°C overnight and then calcined at 500°C for 3 h.

2.2. Hydrogenation of citral

The different catalysts were tested in the citral hydrogenation at 70°C and atmospheric pressure in a discontinuous reactor with a device for sampling the reaction products. In each experiments

0.3 mL of citral (Aldrich, 61% cis and 36% trans) were hydrogenated by using 0.300 g of catalyst and 30 mL of solvent (2-propanol). The reaction mixture was stirred at 1400 rpm (in order to minimize the limitations of the mass transfer steps). In fact, it is worth noticing that from previous experiments, diffusional limitations were found to be absent under these conditions. Prior to the reaction, catalysts were reduced “in-situ” under flowing H_2 at $500^\circ C$ for 3 h, and then they were cooled down to the reaction temperature. The reaction products were analyzed in a GC system coupled to a capillary column (Supelcowax 10M) with a FID detector. All products were identified by using gas chromatography standards except for 3,7-dimethyloctanal. This product was identified by gas chromatography–mass spectrometry (GC–MS) technique. The calculation of the activity and selectivity was made by using the internal normalization methods. The catalytic activity was defined as the sum of percentages of citral converted into different products. The selectivity to a given product (i) was calculated as the ratio between the amount of product i and the total amounts of products.

2.3. Characterization of catalysts

The test reactions of the metallic phase (cyclohexane dehydrogenation – CHD and cyclopentane hydrogenolysis – CPH) were performed in a differential continuous flow reactor at $300^\circ C$. In both reactions the catalysts were previously reduced “in situ” in flowing H_2 at $500^\circ C$ for 3 h and the experiments were performed by using a H_2/CH (or CP) molar ratio equal to 26 and a volumetric flow of 6 mL m^{-1} . The catalyst weight used in these test reaction experiments was such as to obtain a conversion lower than 5% (differential flow reactor model). The reaction products and the remaining reactants were analyzed by using a gas chromatographic system. The activation energy values for CHD (E_{aCH}) were calculated by linear regression using the reaction rates measured at three temperatures (270 , 285 and $300^\circ C$) and the Arrhenius plot ($\ln R^0_{CH}$ versus $1/T$ (K^{-1})).

The H_2 chemisorption measurements were made in a volumetric equipment at room temperature. The sample weight used on the experiments was 0.200 g. In these experiments the catalysts were previously reduced in H_2 at $500^\circ C$ for 3 h, then outgassed under high vacuum (10^{-5} Torr) at the same temperature for 1 h and finally cooled down to room temperature. The H_2 adsorption isotherms were performed at room temperature between 0 and 100 Torr. The isotherms were linear in the range of used pressures and the H_2 chemisorption capacity was calculated by extrapolation of the isotherms to zero pressure [46].

The catalysts were also characterized by temperature programmed reduction (TPR) by using a reductive mixture of H_2 (5%, v/v)– N_2 (10 mL min^{-1}) in a flow reactor. Samples were heated at $6^\circ C\text{ min}^{-1}$ from 25 to $750^\circ C$. Before TPR, samples were calcined “in situ” at $500^\circ C$ for 3 h.

XPS determinations were carried out in a Multitechnic Specs photoemission electron spectrometer equipped with an X-ray source Mg/Al and a hemispherical analyzer PHOIBOS 150 in the fixed analyzer transmission (FAT) mode. The spectrometer operates with an energy power of 100 eV and the spectra were obtained with a pass energy of 30 eV and a Mg anode operated at 100 W. The pressure of the analysis chamber was kept a pressure lower than 5×10^{-8} mbar. Samples were previously reduced under H_2 at $500^\circ C$ for 3 h in a flow reactor and then they were introduced in the equipment and reduced “in situ” with H_2 at $400^\circ C$ for 1 h. The binding energies (BEs) of the signals were referred to the C1s peak at 284 eV. Peak areas and BE values were estimated by fitting the curves with combination of Lorentzian–Gaussian curves of variable proportion using the CasaXPS Peak-fit software version 1.2.

In order to characterize the acidic properties of the supports, the 2-propanol dehydration reaction was used. The reaction was

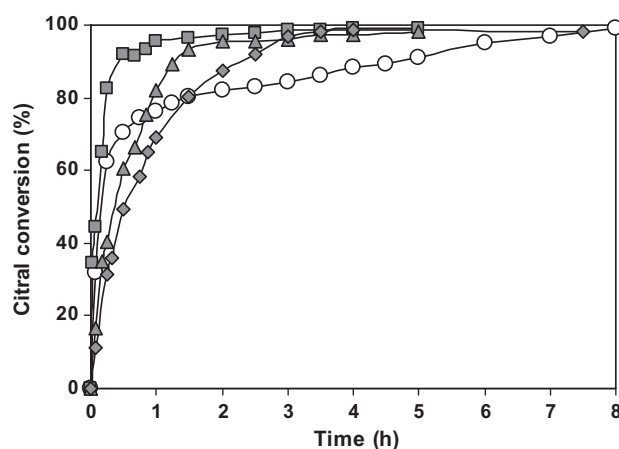


Fig. 2. Citral conversion as a function of the reaction time for the following catalysts: \circ – Pt(5 wt%)/ Al_2O_3 , \blacksquare – Pt(5 wt%)Sn(1 wt%)/ Al_2O_3 , \blacktriangle – Pt(5 wt%)Sn(2 wt%)/ Al_2O_3 and \blacklozenge – Pt(5 wt%)Sn(3 wt%)/ Al_2O_3 .

carried out at $210^\circ C$ in a continuous flow reactor. Samples were previously treated “in situ” under flowing H_2 at $500^\circ C$ for 3 h. The alcohol was vaporized in a H_2 stream ($H_2/2$ -propanol molar ratio = 19) and then it was fed to the reactor with a spacial velocity of $0.52\text{ mol alcohol h}^{-1}\text{ g cat}^{-1}$, the sample weight being 0.100 g in all cases.

3. Results and discussion

3.1. Citral hydrogenation

Fig. 2 shows the total conversion of citral for the Pt/ Al_2O_3 and PtSn/ Al_2O_3 catalyst series as a function of the reaction time. It can be observed that the activities of the bimetallic catalysts are higher than that of the monometallic one after 1.5 h reaction time. This behaviour is in agreement with those reported by other authors [20,25,28,34,47]. Besides, for the bimetallic series, when the Sn loading increases, the activity decreases. In order to clarify the results, θ_{Pt} and θ_{PtSn} parameters were defined, these being the required times to reach a same citral conversion (95%) for monometallic and bimetallic catalysts, respectively. Thus, the relative activity defined as the ratio $\theta_{Pt}/\theta_{PtSn}$ shows that when the Sn amount added to Pt increases from 1 to 3 wt%, it decreases following the sequence: $\theta_{Pt}/\theta_{PtSn} = 6$ for Sn = 1 wt%, 3 for Sn = 2 wt% and 2 for Sn = 3 wt%.

Fig. 3 shows the results of the citral conversion to all products obtained by using Pt/ $MgAl_2O_4$ and PtSn/ $MgAl_2O_4$ catalysts as a function of the reaction time. In this case, the catalytic activity is slightly affected by the Sn loading except for the catalyst with the highest Sn content. It must be noted when compared the results of activity of both catalyst series that catalysts supported on $MgAl_2O_4$ are far more active than those supported on Al_2O_3 .

Figs. 4 and 5 show the selectivity values to different reaction products measured at three citral conversion levels (35, 65 and 95%) for Pt/ Al_2O_3 , Pt/ $MgAl_2O_4$, PtSn/ Al_2O_3 and PtSn/ $MgAl_2O_4$ catalyst series. The names used in these figures are: UA: unsaturated alcohol (geraniol and nerol), CAL: citronella, ISOP: isopulegol, COL: citronellol, MEN: menthol, DA: dimethyloctanal, DO: dimethyl octanol. It can be seen that the monometallic Pt catalysts on both supports (Fig. 4) are selective for unsaturated aldehydes and they display a low formation of unsaturated alcohols.

It can be observed in Fig. 5 that the bimetallic catalysts on both supports display a notorious higher selectivity to unsaturated alcohols than the corresponding monometallic ones. Moreover, it must be noted that the higher the Sn loading added to Pt, the

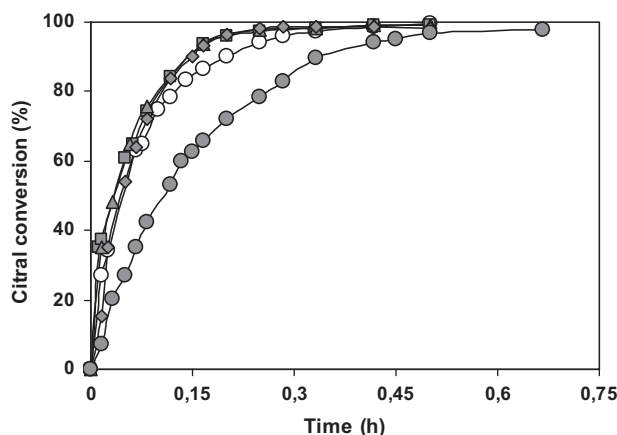


Fig. 3. Citral conversion as a function of the reaction time for the following catalysts: \circ – Pt(5 wt%)/MgAl₂O₄, \blacksquare – Pt(5 wt%)Sn(1 wt%)/MgAl₂O₄, \blacktriangle – Pt(5 wt%)Sn(2 wt%)/MgAl₂O₄ and \blacklozenge – Pt(5 wt%)Sn(3 wt%)/MgAl₂O₄, \bullet – Pt(5 wt%)Sn(4 wt%)/MgAl₂O₄.

higher the selectivity to unsaturated alcohols for both catalyst series, while the selectivities to CAL and COL decrease. These facts indicate that the hydrogenation of the carbonyl group is preferentially favoured with respect to the hydrogenation of double C=C bonds in bimetallic catalysts. Besides, the carbonyl group hydrogenation would probably require a particular site with a given surface structure [17,28]. However, it should also be noted that the effect of the addition of the same Sn loading to the Pt catalysts supported on Al₂O₃ and MgAl₂O₄ does not lead to obtain the same selectivity. Thus, the selectivity to UA for the Pt(5 wt%)Sn(3 wt%)/Al₂O₃ catalyst reaches a value of about 88% while for the Pt(5 wt%)Sn(3 wt%)/MgAl₂O₄ catalyst is lower (65%). Moreover, the addition of higher Sn amounts to Pt catalysts based on MgAl₂O₄ does not enhance significantly the selectivity to UA

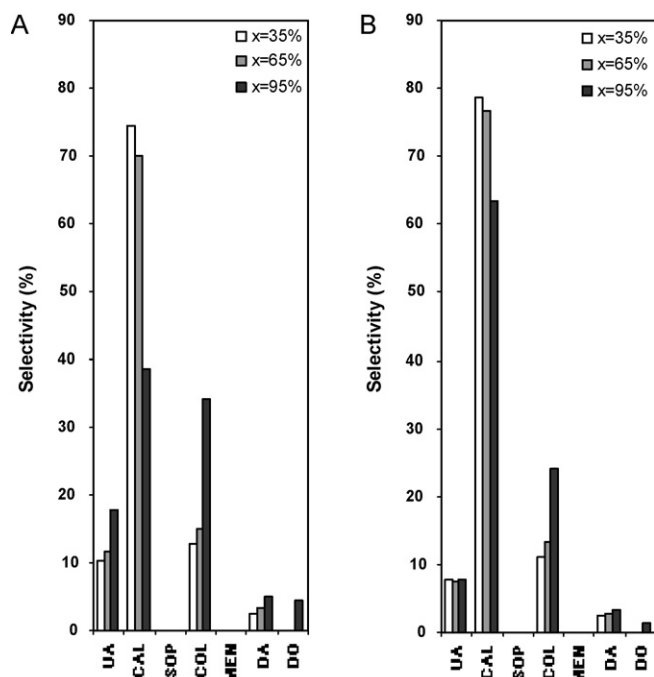


Fig. 4. Selectivities to different products measured at different citral conversion levels: 35, 65 and 95% for monometallic catalysts Pt(5 wt%) supported on Al₂O₃ (A) and MgAl₂O₄ (B). UA: unsaturated alcohol (geraniol and nerol), CAL: citronellal, ISOP: isopulegol, COL: citronellol, MEN: menthol, DA: dimethyloctanal, DO: dimethyloctanol.

Table 1

Selectivity values to different reaction products measured at different reaction time after total conversion of citral for Pt–Sn/Al₂O₃ and Pt–Sn/MgAl₂O₄ catalyst series.

Catalyst	Reaction time (h)	Selectivity (%)			
		UA	CAL	COL	DO
PtSn(1 wt%)/Al ₂ O ₃	2	28.5	0.5	54.5	7.0
PtSn(2 wt%)/Al ₂ O ₃	2	77.2	0	21.6	0
PtSn(3 wt%)/Al ₂ O ₃	2	83.9	0	14.6	0.25
PtSn(1 wt%)/MgAl ₂ O ₄	4	–	–	–	100
PtSn(3 wt%)/MgAl ₂ O ₄	4	–	–	–	100
PtSn(4 wt%)/MgAl ₂ O ₄	4	–	–	–	100

since the selectivity value for Pt(5 wt%)Sn(4 wt%)/MgAl₂O₄ catalyst is of about 73% this being lower than the one showed by Pt(5 wt%)Sn(3 wt%)/Al₂O₃. Then, it is the nature of support that produces noticeable differences both on the catalytic activity and selectivity.

On the other hand, it was observed during the reaction that the formation of citronellol is mainly produced by the citronellal hydrogenation in the monometallic catalysts, while for bimetallic catalysts the citronellol formation is due to not only the citronellal hydrogenation but also the hydrogenation of unsaturated alcohols. This effect is more important for the bimetallic catalysts with low Sn loading supported on Al₂O₃ and in all the PtSn/MgAl₂O₄ catalytic series. In these cases, the amount of citronellol, when all citronellal was consumed, increases because the route of hydrogenation of unsaturated alcohols to citronellol remains active. Besides, the experiments showed that this hydrogenation step continues towards the formation of dimethyloctanol for these catalysts after the total citral conversion. In fact, Table 1 shows the selectivity values to different reaction products measured at different reaction time after citral was completely consumed in the reaction medium for PtSn/Al₂O₃ and PtSn/MgAl₂O₄ catalyst series. It is observed for PtSn/MgAl₂O₄ catalysts that after 4 h reaction time (after the total citral conversion), the different compounds are completely hydrogenated and converted into dimethyloctanol. For bimetallic catalysts supported on alumina, at 2 h reaction time (after the total citral conversion), the selectivity to unsaturated alcohols of PtSn(1 wt%)/Al₂O₃ catalyst markedly decreases with respect to that at 95% citral conversion, while the selectivities to COL and DO increase. Additionally, it must be noted in Fig. 5 that, when the citral conversion increases from 65 to 95%, the selectivity to unsaturated alcohols in bimetallic catalysts supported on Al₂O₃ with low Sn content (1 wt%) decreases too. In the case of bimetallic catalysts supported on Al₂O₃ with Sn amount >1 wt%, it can be observed in Table 1 that the selectivity to UA at 2 h reaction time (after the total citral conversion) slightly decreases with respect to the values corresponding to PtSn(2 wt%)/Al₂O₃ and PtSn(3 wt%)/Al₂O₃ catalysts, respectively, at 95% of citral conversion (see Fig. 5B and C). In this sense, for these catalysts, results show that both the transformation rate of unsaturated alcohols into citronellol and the dimethyloctanol formation appear to be slower than those corresponding to the other catalysts. These facts indicate that the selective hydrogenation of the carbonyl group and the inhibition of the hydrogenation of the C=C bonds of citral would require a given surface structure of the reaction sites [17,20].

From the above mentioned results related to the catalytic activity in the citral hydrogenation, it was concluded that the metallic phases and probably the density of the reaction sites for the hydrogenation of the C=O and C=C bonds in both catalytic series are very different. Besides, these results would indicate that the different catalytic behaviours of the metallic phase of monometallic and bimetallic catalysts of both series could also be due to the support effect.

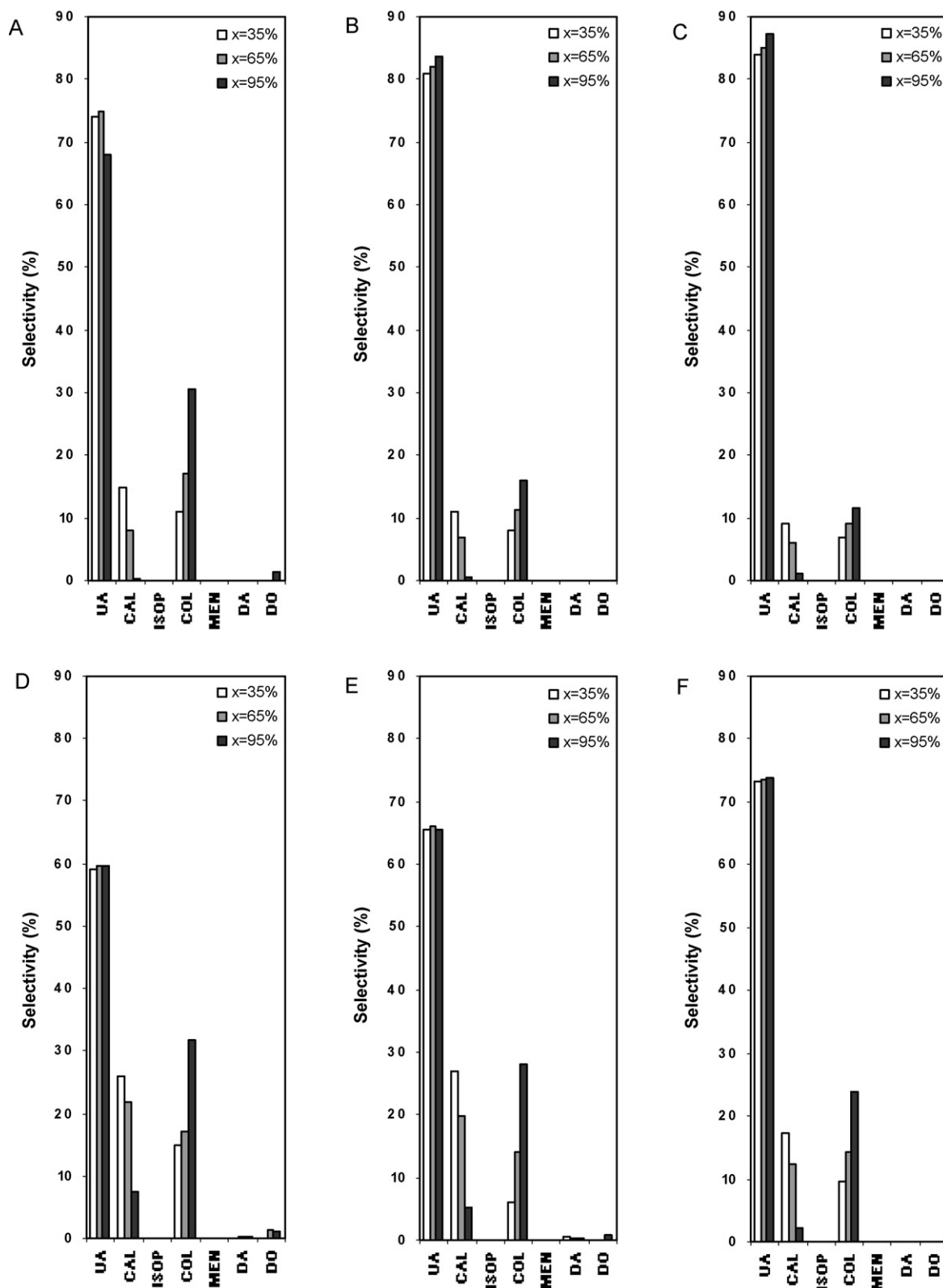


Fig. 5. Selectivities to different products measured at different citral conversion levels, 35, 65 and 95%, for different bimetallic catalysts: (A) PtSn(1 wt%)/Al₂O₃, (B) PtSn(2 wt%)/Al₂O₃, (C) PtSn(3 wt%)/Al₂O₃, (D) PtSn(1 wt%)/MgAl₂O₄, (E) PtSn(3 wt%)/MgAl₂O₄ and (F) PtSn(4 wt%)/MgAl₂O₄. UA: unsaturated alcohol (geraniol and nerol), CAL: citronellal, ISOP: isopulegol, COL: citronellol, MEN: menthol, DA: dimethyloctanal, DO: dimethylctanol.

Furthermore, it is very important to note the absence of cyclization products (isopulegol and menthol) for both catalyst series [48]. This fact is expected for catalysts supported on MgAl₂O₄ due to the neutral character of this material, but not for catalysts supported

on Al₂O₃, where the support has an acidic character [49,50]. Fig. 6 shows the 2-propanol dehydration conversion (as a measurement of the total acid character of the support [45]) as a function of the reaction time for Al₂O₃ and MgAl₂O₄ supports. It can be observed

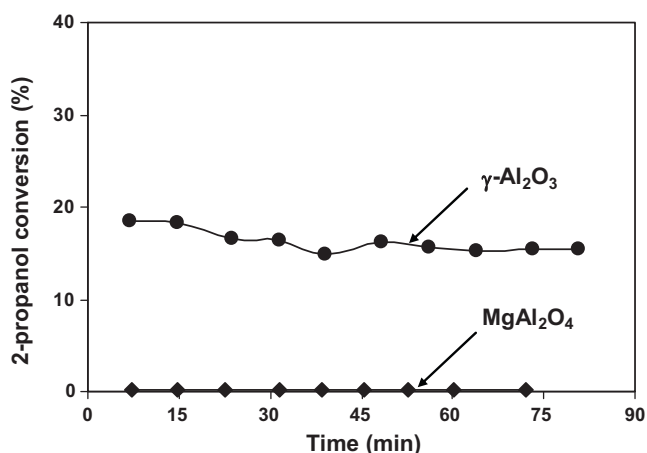


Fig. 6. 2-Propanol conversion versus time for Al_2O_3 and MgAl_2O_4 .

that alumina has a higher acidic character than MgAl_2O_4 . However, the acidic strength of the alumina is not enough to catalyze the cyclization reaction. It should be remarked that Sn produces an additional poisoning effect on the acidic centers of the support [51].

3.2. Catalyst characterization

3.2.1. Test reactions of the metallic phase and H_2 chemisorption

Table 2 shows the values of the initial rates of cyclohexane dehydrogenation (R_{CH}^0) and cyclopentane hydrogenolysis (R_{CP}^0) for both catalyst series. The values of activation energy in CHD (E_{aCH}) and the H_2 chemisorption capacity (H) are also included.

The CHD is a structure-insensitive reaction [52], which is carried out on the surface active atoms of the catalyst. In this reaction the activation energy will not be modified if the nature of the metallic site is not changed by any other effect (for example the addition of a second metal). Hence any modification in the activation energy values is caused by an electronic modification in the metal–metal interaction or a change of the metallic phase structure. The results of the CHD show that the Sn addition to $\text{Pt}/\text{Al}_2\text{O}_3$ catalyst leads to an important increment of the activation energy (from 22 to 45 kcal mol^{-1}) and to a decrease of the initial reaction rate (this decrease is higher than one order of magnitude with respect to the value of the monometallic catalyst). These results clearly indicate an important electronic modification of the active phase by Sn with probable alloy formation in bimetallic catalysts supported on Al_2O_3 .

In the case of bimetallic catalysts supported on MgAl_2O_4 it can be observed that the initial reaction rate of CHD slightly decreases when increasing Sn amounts are added to Pt (Table 2). The activation energy values increase in lower proportion (with respect to the monometallic sample) than those for $\text{PtSn}/\text{Al}_2\text{O}_3$ catalysts.

Taking into account the structure-insensitive character of the CHD, it can be inferred that there is not practically electronic effect in $\text{PtSn}/\text{MgAl}_2\text{O}_4$ catalysts.

The CPH is a structure-sensitive reaction [53], which is carried out on ensembles of a certain number of active atoms. This means that the modification of the reaction rate by addition of a second metal to the active metal can break the metallic ensembles necessary for the reaction. Table 2 shows that the addition of 1 wt% of Sn to Pt supported on Al_2O_3 produces a significant decrease of the reaction rate, but the addition of higher Sn amounts completely inhibits the reaction. In consequence, this means that Sn addition to $\text{Pt}/\text{Al}_2\text{O}_3$ produces not only an electronic effect but also a geometric one [34] since there is a decrease of the concentration of metallic ensembles necessary to carry out the hydrogenolysis reaction, probably due the deposition of Sn in the vicinity of Pt.

Table 2 also shows the initial reaction rates in CPH for the catalysts supported on MgAl_2O_4 . It is observed that the reaction rate decreases in an important way in bimetallic catalysts with respect to the monometallic one, though this decrease is lower than that corresponding to bimetallic catalysts supported on Al_2O_3 when increasing Sn amounts are added to Pt.

It is also observed a marked diminution of the H_2 chemisorption values (Table 2) when increasing Sn amounts are added to Pt in both catalytic series. These results are in agreement with the results of the test reactions. For catalysts based on Al_2O_3 , this behaviour can probably be due to a modification of the electronic structure of the metallic phase [54,55], and also the existence of geometric effects (dilution or blocking of Pt by Sn). However considering the CHD and CPH results, for catalysts based on MgAl_2O_4 , it is mainly the presence of geometric effects that would produce the diminution of the H_2 chemisorption values in these bimetallic catalysts.

The Pt dispersion values, calculated from the chemisorption data shown in Table 1, are 33.4% for $\text{Pt}/\text{Al}_2\text{O}_3$ and 25.3% for $\text{Pt}/\text{MgAl}_2\text{O}_4$. Then, as expected, the TON value (defined as $R_{\text{CH}}^0/\text{Pt dispersion}$) in CHD for the monometallic catalyst supported on MgAl_2O_4 (39.8 $\text{mol CHD h}^{-1} \text{g}^{-1}$ of exposed Pt) is lower than the one corresponding to the monometallic catalyst supported on Al_2O_3 (52.7 $\text{mol CHD h}^{-1} \text{g}^{-1}$ of exposed Pt). However, in spite of the lower dispersion found for $\text{Pt}/\text{MgAl}_2\text{O}_4$ catalyst, the specific activity in the citral hydrogenation reaction was clearly higher for this catalyst than for $\text{Pt}/\text{Al}_2\text{O}_3$ one. These results would indicate that the different catalytic behaviours in CHD and citral hydrogenation of the metallic phase of both monometallic catalysts could be due not only to the support effect but also to the existence of a different accessibility of the reactants (citral and CH) towards the active sites.

In conclusion the above mentioned results clearly show the differences in the structure of the metallic phase of monometallic and bimetallic catalysts according to the used support (Al_2O_3 or MgAl_2O_4). The different catalytic behaviours when increasing amounts of Sn are added to Pt could be related to the presence of different species of Sn (ionic, zerovalent), which could be intercalated among Pt atoms and could be partially blocking them in

Table 2

Initial reaction rates of CHD (R_{CH}^0) and CPH (R_{CP}^0), activation energy in CDH (E_{aCH}) and H_2 chemisorption capacity (H) for different catalysts.

Catalyst	R_{CH}^0 ($\text{mol h}^{-1} \text{g}^{-1} \text{Pt}$)	E_{aCH} (kcal mol^{-1})	R_{CP}^0 ($\text{mol}^{-1} \text{h}^{-1} \text{g}^{-1} \text{Pt}$)	H ($\mu\text{mol/g catal}$)
$\text{Pt}/\text{Al}_2\text{O}_3$	17.6	22	2.14	42.6
$\text{PtSn}(1 \text{ wt}\%)/\text{Al}_2\text{O}_3$	5.4	25	0.02	14.8
$\text{PtSn}(2 \text{ wt}\%)/\text{Al}_2\text{O}_3$	0.5	36	n.m.	7.7
$\text{PtSn}(3 \text{ wt}\%)/\text{Al}_2\text{O}_3$	0.1	45	n.m.	3.1
$\text{Pt}/\text{MgAl}_2\text{O}_4$	9.9	21	2.25	32.3
$\text{PtSn}(1 \text{ wt}\%)/\text{MgAl}_2\text{O}_4$	5.9	22	0.12	13.4
$\text{PtSn}(2 \text{ wt}\%)/\text{MgAl}_2\text{O}_4$	6.4	23	0.08	6.6
$\text{PtSn}(3 \text{ wt}\%)/\text{MgAl}_2\text{O}_4$	5.1	25	0.06	3.5
$\text{PtSn}(4 \text{ wt}\%)/\text{MgAl}_2\text{O}_4$	4.6	26	0.04	3.3

n.m.: not measurable.

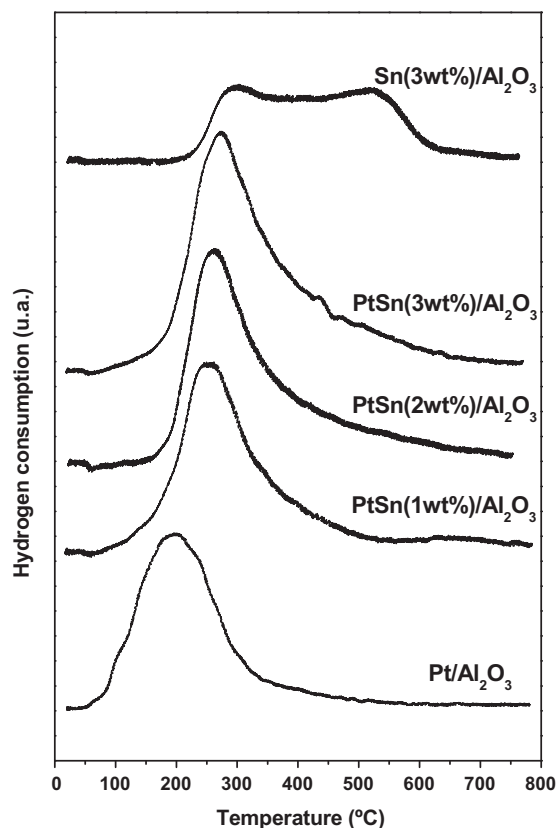


Fig. 7. TPR profiles for Sn(3 wt%)/Al₂O₃, Pt(5 wt%)/Al₂O₃ and Pt(5 wt%)Sn/Al₂O₃ with Sn contents of 1, 2 and 3 wt%.

a different proportion. Besides, the formation of PtSn alloys could produce an electronic modification of the metallic phase. According to the catalyst type, the structure of the metallic phase produced by Sn addition could favour the hydrogenation of the carbonyl group. In this sense, the presence of electronic or/and geometric effects of Sn species on the metallic phase appears to be not only more pronounced for PtSn/Al₂O₃ catalysts (which display a significant change of the E_{aCH} , and a higher decrease both of H₂ chemisorption and CPH reaction rates than the PtSn/MgAl₂O₄ ones) but also more suitable to conform a better structure of the metallic phase for the hydrogenation of the carbonyl group.

3.2.2. TPR profiles

Other evidence of a better Pt–Sn interaction in catalysts supported on Al₂O₃ were observed from TPR results. Fig. 7 shows the TPR profiles for the PtSn/Al₂O₃ catalyst series. For the sake of comparison the TPR profiles of the monometallic catalysts (Pt(5 wt%)/Al₂O₃ and Sn(3 wt%)/Al₂O₃) are also included. Pt/Al₂O₃ catalyst shows a reduction peak with a maximum at about 200–210 °C, while Sn(3 wt%)/Al₂O₃ presents a broad reduction zone between 240 and 600 °C. Bimetallic PtSn/Al₂O₃ catalysts show only one reduction peak similar to monometallic catalyst. These peaks in bimetallic catalysts are broader than that of Pt/Al₂O₃ catalyst and they are shifted to higher temperatures as the Sn loading increases (maximums at about 250, 260 and 270 °C for catalysts with 1, 2 and 3 wt% of Sn, respectively) with respect to that of the monometallic Pt catalyst. It is observed a certain reduction zone at temperatures higher than 400 °C (temperature zone where the reduction of free Sn stabilized on the support takes place), this showing the presence of Sn species on the support. These findings can be understood as a co-reduction of both metals (Pt and Sn) with probable alloy formation, which is in agreement with the increment of activation energy

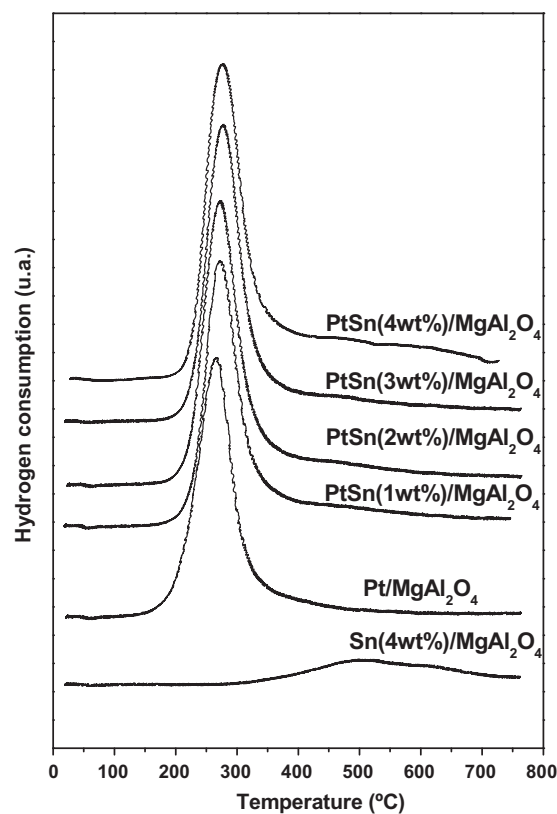


Fig. 8. TPR profiles of Pt(5 wt%)/MgAl₂O₄, Sn(4 wt%)/MgAl₂O₄ and Pt(5 wt%)Sn/MgAl₂O₄ catalysts with different Sn contents.

values observed in CHD. The broadening of the reduction peaks in bimetallic catalysts could be due to the existence of different metallic species and the presence of Sn species in the vicinity of Pt. These effects appear to be more important as the Sn loading increases.

Fig. 8 displays the TPR profiles for the PtSn/MgAl₂O₄ catalyst series. The TPR profiles of the monometallic Pt(5 wt%)/MgAl₂O₄ and Sn(4 wt%)/MgAl₂O₄ catalysts are also included. Sn(4 wt%)/MgAl₂O₄ catalyst shows a very small and broad reduction zone between 400 and 700 °C. In contrast with the bimetallic catalysts supported on Al₂O₃, PtSn/MgAl₂O₄ catalysts show only one important reduction peak at about 275 °C, this temperature being similar to that found in the Pt(5 wt%)/MgAl₂O₄. In all series of bimetallic catalysts supported on MgAl₂O₄ it is observed that there are no shifts in the temperature of this reduction peak and the H₂ consumption values up to 400 °C are similar, which indicates that the first peak corresponds to the reduction of Pt species in all bimetallic catalysts and a small Pt–Sn coreduction. Moreover, it must be noted that all bimetallic catalysts, mainly those with higher Sn loadings show a small reduction zone at temperatures higher than 400 °C. All these results would indicate a co-reduction of Pt and Sn, but with low alloy formation (in agreement with the activation energy values found for CHD), and probably with a certain fraction of free Sn species stabilized on the support.

3.2.3. XPS measurements

In order to determinate the oxidation state of the different metals in the monometallic and bimetallic catalysts after the reduction at 500 °C, XPS experiments were carried out. From Pt4d spectra of these samples, the presence of only one peak (at about 313.6–314.8 eV) in all catalysts was found. This peak can be assigned to Pt⁰ [56,57]. Fig. 9 shows the Sn3d_{5/2} XPS spectra for PtSn(1 wt%)/Al₂O₃ and PtSn(3 wt%)/Al₂O₃ catalysts and Fig. 10 shows the Sn3d_{5/2} XPS spectra for PtSn(1 wt%)/MgAl₂O₄

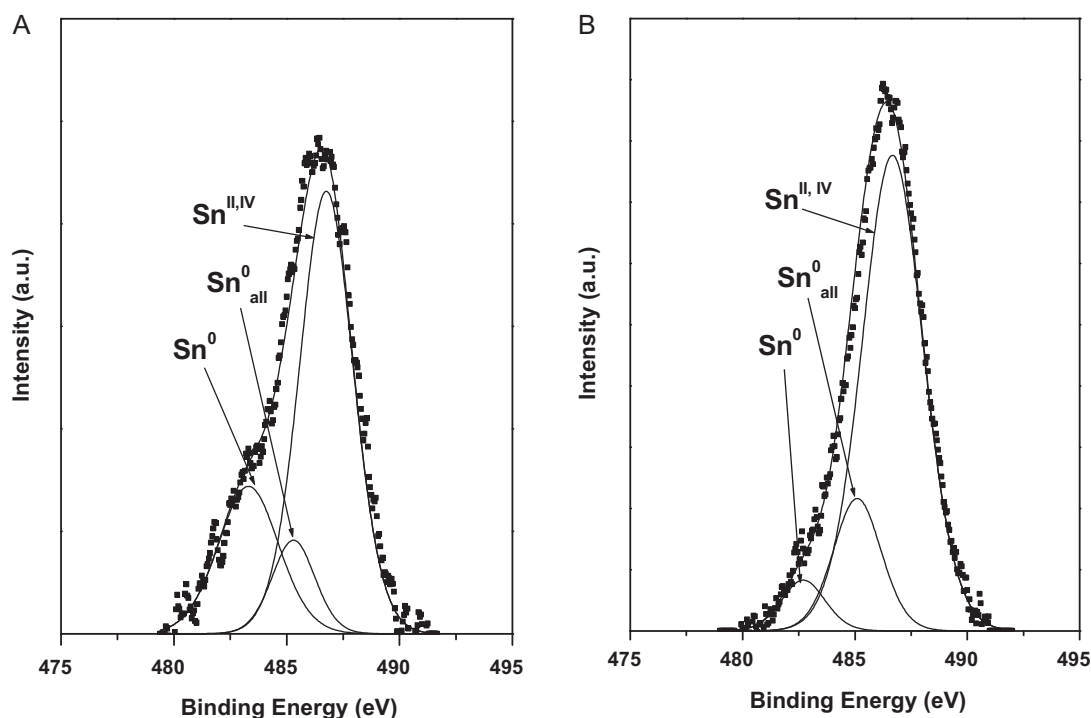


Fig. 9. $\text{Sn}3d_{5/2}$ XPS profiles for (a) $\text{Pt}(5 \text{ wt}\%)\text{Sn}(1 \text{ wt}\%)/\text{Al}_2\text{O}_3$ and (b) $\text{Pt}(5 \text{ wt}\%)\text{Sn}(3 \text{ wt}\%)/\text{Al}_2\text{O}_3$ samples.

and $\text{PtSn}(4 \text{ wt}\%)/\text{MgAl}_2\text{O}_4$ ones. In the case of bimetallic catalysts supported on Al_2O_3 , the $\text{Sn}3d_{5/2}$ XPS profiles are more complex than those corresponding to $\text{PtSn}/\text{MgAl}_2\text{O}_4$ catalysts. Taking into account the shape and the width of the profiles (for catalysts supported on Al_2O_3), they were deconvoluted in three peaks: the first one at about 482.7–483.3 eV which can be assigned to Sn^0 , the peak at about 485.1–485.3 eV that can be due to the presence of alloyed Sn (Sn_{all}) [23,58,59], and the third peak located at about 486.7–486.8 eV, which is the major one and it can be attributed to oxidized Sn species [20,29]. The peak assignment was made con-

sidering the results reported by Homs et al. [58,59] who found Sn^0 , Sn_{all} and oxidized Sn ($\text{Sn}^{\text{II,IV}}$) in bimetallic $\text{PtSn}/\text{Al}_2\text{O}_3$ and PtSn/SiO_2 catalysts by using XPS, EXAFS, TEM and XRD. In this sense, our results of CHD support the XPS results since they indicate an electronic modification of the metallic phase due to the activation energy values clearly increase when Sn is added to Pt.

For the $\text{PtSn}/\text{MgAl}_2\text{O}_4$ catalysts, the deconvolution of the $\text{Sn}3d_{5/2}$ XPS profiles was carried out in two peaks: one at about 482.3–483.0 eV and the other one at about 485.4–485.7 eV. The first peak was assigned to Sn^0 [20,29], while the second one was

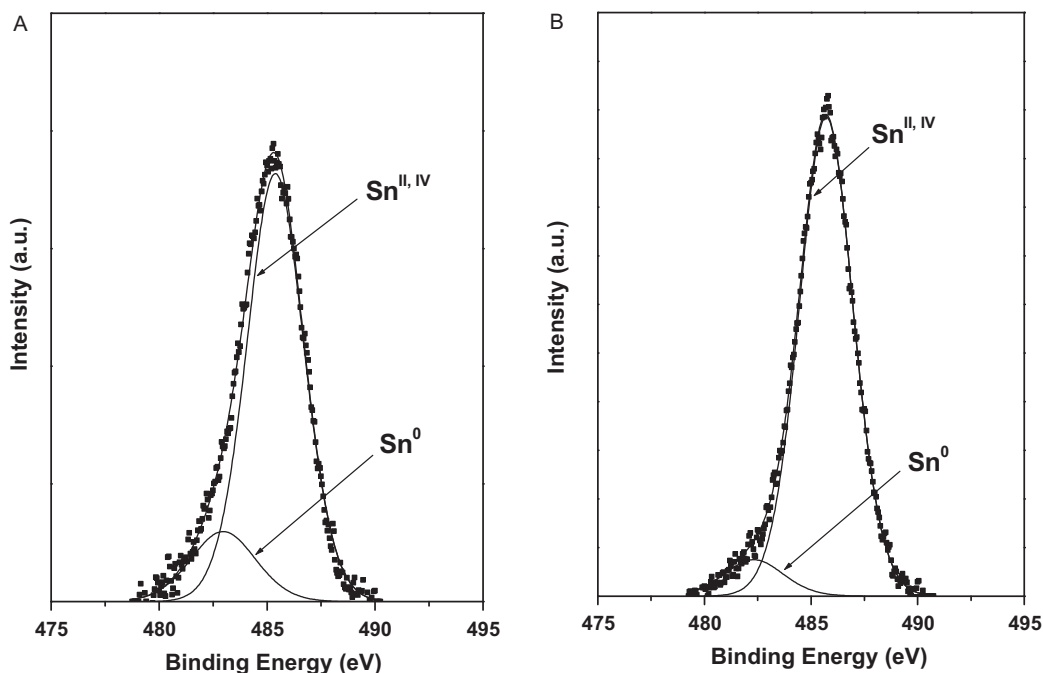


Fig. 10. $\text{Sn}3d_{5/2}$ XPS profiles for (a) $\text{Pt}(5 \text{ wt}\%)\text{Sn}(1 \text{ wt}\%)/\text{MgAl}_2\text{O}_4$ and (b) $\text{Pt}(5 \text{ wt}\%)\text{Sn}(4 \text{ wt}\%)/\text{MgAl}_2\text{O}_4$ samples.

Table 3
XPS results of different catalysts corresponding to Pt4d_{5/2} and Sn3d_{5/2} levels.

Catalyst	BE (eV) Pt4d _{5/2} level; species (%)	BE (eV) Sn3d _{5/2} level; species (%)	Bulk Sn _T /Pt atomic ratio	Surface Sn _T /Pt atomic ratio
Pt/Al ₂ O ₃	314.5; Pt(0); 100%	–	–	–
PtSn(1 wt%)/Al ₂ O ₃	314.8; Pt(0); 100%	483.3; Sn(0); 24.4%; 485.3; Sn(alloy); 11.0%; 486.8; Sn(II,IV); 64.7%	0.33	1.66
PtSn(3 wt%)/Al ₂ O ₃	314.4; Pt(0); 100%	482.7; Sn(0); 5.9%; 485.1; Sn(alloy); 16.9%; 486.7; Sn(II,IV); 77.2%	0.99	4.43
Pt/MgAl ₂ O ₄	313.8; Pt(0); 100%	–	–	–
PtSn(1 wt%)/MgAl ₂ O ₄	313.6; Pt(0); 100%	483.0; Sn(0); 15.8% 485.4; Sn(II,IV); 84.2%	0.33	1.26
PtSn(4 wt%)/MgAl ₂ O ₄	314.1; Pt(0); 100%	482.3; Sn(0); 7.7% 485.7; Sn(II,IV); 92.3%	1.33	1.88

attributed to oxidized species of Sn^{II,IV}, since according to the literature Sn^{II} and Sn^{IV} cannot be discriminated because their binding energies are very similar [60].

Table 3 displays the BE and the percentage of Sn⁰ and oxidized Sn, the Sn_T/Pt molar ratio in the bulk (Sn_T: total moles of Sn) and the (Sn/Pt)_{surface} (surface molar ratio) obtained from XPS experiments on the different catalysts. The presence of small quantities of Sn⁰ in bimetallic catalysts supported on MgAl₂O₄ indicates the low Sn reducibility degree in these catalysts. It should be noted that these results are in agreement with those found by TPR measurements. On the other hand, taking into account the TPR and XPS results for bimetallic catalysts supported on Al₂O₃, it can be concluded that a certain amount of Sn is present as Sn⁰, other Sn amount as Sn_{all} and the remaining Sn fraction as oxidized species. Besides, the presence of Sn in the zerovalent state decreases as its content increases for both catalyst series (see Table 3). Moreover, in the case of bimetallic catalysts based on Al₂O₃ the fraction of alloyed Sn increases when the Sn loading increases. By comparing the values of (Sn/Pt)_{surface} with those of (Sn_T/Pt)_{bulk} it can be concluded that there is a surface enrichment of the metallic surface by Sn in both catalyst series, this enrichment being higher in catalysts based on Al₂O₃.

In conclusion, XPS results indicate that the structure of metallic phase is modified by the nature of the support and the promoter (Sn) loading, in agreement with those results obtained from other characterization techniques. However, XPS measurements also allow to determine with more details the nature of the metallic surface. Then, the differences found in the catalytic behaviour for bimetallic catalysts supported on Al₂O₃ and MgAl₂O₄ can be better explained on the basis of the different metallic surface structures. According to the literature, the oxidized Sn species in the catalytic surface are responsible for the polarization of the carbonyl group [17,18,20] and the consequent increment of the hydrogenation rate of this group leading to unsaturated alcohols. These effects together with the partial dilution of Pt by Sn species could increase the selectivity to unsaturated alcohols of bimetallic catalysts with respect to monometallic Pt ones. It should be noted that Sn can be present in the metallic phase as Sn⁰ or forming PtSn alloys in some cases. In both cases (Sn⁰ alone or PtSn alloys) the Sn would also contribute to the dilution effect [17,23]. Besides, the PtSn alloys could be active for the hydrogenation of –C=C– groups and for the polarization of the carbonyl group. In this sense, several authors studied the adsorption of α,β-unsaturated aldehydes by means of density functional calculations and high-resolution photoelectron spectroscopy on well-defined PtSn alloys and Pt(1 1 1) surfaces [31,32,61,62]. They reported that for the most stable possible adsorption structures of α,β-unsaturated aldehydes, the adsorption energy is smaller on the alloys than on platinum, but they also observed that on the alloys there is an enhancement to the relative stability of adsorption structures which leads to the hydrogenation of carbonyl group. According to our characterization results, the state of the metallic phase in bimetallic catalysts of both series is strongly influenced by both the nature of the support and the Sn addition (geometric and electronic effects). In this sense, XPS results show that an important fraction of Sn is found as oxidized Sn, which explains the important values of selectivity to

UA in both catalyst series (Fig. 5). However, not only this effect but also the electronic one must be taken into account to explain the higher selectivity of PtSn supported on Al₂O₃ than those supported on MgAl₂O₄. In fact, in PtSn/Al₂O₃ catalysts, PtSn alloyed particles would inhibit the hydrogenation of the olefinic bond probably due to the additional dilution effect and on the other hand would they enhance the hydrogenation of the carbonyl group because this group could be preferentially adsorbed over the alloyed surface. It must be noted that the presence of alloys in these catalysts was observed by XPS and inferred from test reaction (CHD). Besides, the additional dilution effect produced by the alloy particles is in agreement with the lower hydrogenolytic capacity found for PtSn/Al₂O₃ catalysts with respect to PtSn/MgAl₂O₄ ones.

4. Conclusions

The citral hydrogenation was studied by using Pt and PtSn catalysts supported on Al₂O₃ and MgAl₂O₄ and using mild reaction conditions. It has been found that for both catalyst series when the Sn loading added to Pt increases, the selectivity to unsaturated alcohols it also enhanced, the alumina support giving the best selectivity to UA. Thus, PtSn(3 wt%)/Al₂O₃ catalyst displays the highest selectivity value to UA (88%) while PtSn(3 wt%)/MgAl₂O₄ and PtSn(4 wt%)/MgAl₂O₄ catalysts show a lower selectivity values (65 and 73%, respectively). According to the characterization results, it can be inferred that the metallic phase in bimetallic catalysts is strongly affected by the tin addition and the nature of the support. In this sense, for the catalysts supported on alumina, both dilution and electronic effects were found, while for samples supported on MgAl₂O₄ mainly geometric effects appear to take place. The presence of oxidized Sn species in both catalyst series would favour the polarization of the carbonyl group thus increasing the selectivity to UA. The presence of alloyed particles in catalysts supported on Al₂O₃ would increase the selectivity values to unsaturated alcohols probably due to an additional dilution effect of Pt by Sn⁰ species and they could also increase the hydrogenation of carbonyl group. In this sense, the high Pt–Sn interaction in PtSn/Al₂O₃ catalysts seems to have a positive effect for obtaining a high selectivity to the unsaturated alcohols.

Acknowledgements

Authors thank Miguel A. Torres and Julieta P. Stassi for the experimental assistance. This work was made with the financial support of ANPCYT and Universidad Nacional del Litoral (Project CAI+D) – Argentina.

References

- [1] P. Gallezot, A. Giroir-Fendler, D. Richard, in: W. Pascoe (Ed.), *Catalysis of Organic Reactions*, Marcel Dekker, New York, 1991, pp. 1–17.
- [2] F.V. Wells, M. Billot, *Perfumery Technology*, E. Horwood Publishers, Chichester, UK, 1981, p. 149.
- [3] G.V. Smith, F. Notheisz, *Heterogeneous Catalysis in Organic Chemistry*, Academic Press, London, 1999, pp. 58–64.

- [4] Ullmann's Encyclopedic of Industrial Chemistry, vol. 14, sixth ed., Wiley-VCH, Weinheim, 2003, p. 123.
- [5] P. Mäki-Arvela, J.G. Hájek, T. Salmi, D.Y. Murzin, *Appl. Catal. A: Gen.* 292 (2005) 1–49.
- [6] P. Claus, *Top. Catal.* 5 (1998) 51–62.
- [7] R. Touroude, *J. Catal.* 65 (1980) 110–120.
- [8] P. Gallezot, D. Richard, *Catal. Rev. Sci. Eng.* 40 (1998) 81–126.
- [9] U.K. Singh, M.A. Vannice, *J. Catal.* 199 (2001) 73–84.
- [10] V. Ponec, *Appl. Catal. A: Gen.* 149 (1997) 27–48.
- [11] U.K. Singh, M.A. Vannice, *Appl. Catal. A: Gen.* 213 (2001) 1–24.
- [12] P. Kluson, L. Cervený, *Appl. Catal. A: Gen.* 128 (1995) 13–31.
- [13] C. Mohr, P. Claus, *Sci. Progress* 84 (2001) 311–334.
- [14] B. Coq, F. Figueras, *Coord. Chem. Rev.* 178–180 (1998) 1753–1783.
- [15] T.B.L.W. Marinelli, S. Nabuurs, V. Ponec, *J. Catal.* 151 (1995) 431–438.
- [16] M. Englich, V.S. Ranade, J.A. Lercher, *J. Mol. Catal. A: Chem.* 121 (1997) 69–80.
- [17] N. Homs, J. Llorca, P. de la Piscina, F. Rodríguez-Reinoso, A. Sepúlveda-Escribano, J. Silvestre-Albero, *Phys. Chem. Chem. Phys.* 3 (2001) 1782–1788.
- [18] S. Galvagno, C. Milone, A. Donato, G. Neri, R. Pietropaolo, *Catal. Lett.* 18 (1993) 349–355.
- [19] J.L. Margitfalvi, A. Tompos, I. Kolosova, J. Valyon, *J. Catal.* 174 (1998) 246–249.
- [20] I.M.J. Vilella, S.R. de Miguel, C. Salinas-Martínez de Lecea, A. Linares-Solano, O. Scelza, *Appl. Catal. A: Gen.* 281 (2005) 247–258.
- [21] I.M. Vilella, I. Borbáth, J.L. Margitfalvi, K. Lázár, S.R. de Miguel, O.A. Scelza, *Appl. Catal. A: Gen.* 326 (2007) 37–47.
- [22] I.M.J. Vilella, S.R. de Miguel, O.A. Scelza, *J. Mol. Catal. A: Chem.* 284 (2008) 161–171.
- [23] F. Coloma, J. Llorca, N. Homs, P. Ramírez de la Piscina, F. Rodríguez-Reinoso, A. Sepúlveda-Escribano, *Phys. Chem. Chem. Phys.* 2 (2000) 3063–3069.
- [24] F. Coloma, A. Sepúlveda-Escribano, J.L.G. Fierro, F. Rodríguez-Reinoso, *Appl. Catal. A: Gen.* 136 (1996) 231–248.
- [25] F. Coloma, A. Sepúlveda-Escribano, J.L.G. Fierro, F. Rodríguez-Reinoso, *Appl. Catal. A: Gen.* 148 (1996) 63–80.
- [26] D.I. Jerdev, A. Olivas, B.E. Koel, *J. Catal.* 205 (2002) 278–288.
- [27] G. Neri, C. Milone, S. Galvagno, A.P.J. Pijpers, J. Schwank, *Appl. Catal. A: Gen.* 227 (2002) 105–115.
- [28] G. Neri, C. Milone, A. Donato, L. Mercadante, A.M. Visco, *J. Chem. Technol. Biotechnol.* 60 (1994) 83–88.
- [29] S.R. de Miguel, M.C. Román-Martínez, E.L. Jablonski, J.L. Fierro, D. Cazorla-Amorós, O.A. Scelza, *J. Catal.* 184 (1999) 514–525.
- [30] J.C. Serrano-Ruiz, G.W. Huber, M.A. Sánchez-Castillo, J.A. Dumesic, F. Rodríguez-Reinoso, A. Sepúlveda-Escribano, *J. Catal.* 241 (2006) 378–388.
- [31] F. Delbecq, P. Sautet, *J. Catal.* 220 (2003) 115–126.
- [32] E. Janin, H. von Schenck, S. Ringler, J. Weissenrieder, T. Akermark, M. Göthelid, *J. Catal.* 215 (2003) 245–253.
- [33] S.R. de Miguel, M.C. Román-Martínez, D. Cazorla-Amorós, E.L. Jablonski, O.A. Scelza, *Catal. Today* 66 (2001) 289–295.
- [34] G.C. Torres, S.D. Ledesma, E.L. Jablonski, S.R. de Miguel, O.A. Scelza, *Catal. Today* 48 (1999) 65–72.
- [35] M. Arai, H. Takahashi, M. Shirai, Y. Nishiyama, T. Ebina, *Appl. Catal. A: Gen.* 176 (1999) 229–237.
- [36] M.A. Vannice, B. Sen, *J. Catal.* 115 (1989) 65–78.
- [37] M. Abid, F. Ammari, K. Liberková, R. Touroude, *Stud. Surf. Sci. Catal.* 145 (2003) 267–270.
- [38] I. Kun, G. Szöllösi, M. Bartók, *J. Mol. Catal. A: Chem.* 169 (2001) 235–246.
- [39] J.C.S. Wu, W.-C. Chen, *Appl. Catal. A: Gen.* 289 (2005) 179–185.
- [40] P. Mäki-Arvela, N. Kumar, K. Eränen, T. Salmi, D.Y. Murzin, *Chem. Eng. J.* 122 (2006) 127–134.
- [41] J. Kijenski, P. Winiarek, T. Paryjczak, A. Lewicki, A. Mikoljska, *Appl. Catal. A: Gen.* 233 (2002) 171–182.
- [42] M. von Arx, T. Mallat, A. Baiker, *J. Mol. Catal. A: Chem.* 148 (1999) 275–283.
- [43] B. Coq, F. Figueras, P. Geneste, U.C. Moreau, P. Moreau, M. Warawdekar, *J. Mol. Catal. A: Chem.* 78 (1993) 211–226.
- [44] A.J. Marchi, D.A. Gordo, A.F. Trasarti, C.R. Apesteguía, *Appl. Catal. A: Gen.* 249 (2003) 53–67.
- [45] S.A. Bocanegra, A.D. Ballarini, O.A. Scelza, S.R. de Miguel, *Mat. Chem. Phys.* 111 (2008) 534–541.
- [46] J.E. Benson, M. Boudart, *J. Catal.* 4 (1965) 704–710.
- [47] S. Galvagno, C. Milone, A. Donato, G. Neri, R. Pietropaolo, *Catal. Lett.* 17 (1993) 55–61.
- [48] A.F. Trasarti, A.J. Marchi, C.R. Apesteguía, *J. Catal.* 224 (2004) 484–488.
- [49] H. Pines, W.O. Haag, *J. Am. Chem. Soc.* 82 (1960) 2471–2483.
- [50] P.J. Kropp, G.W. Breton, S.L. Craig, S.D. Crawford, W.F. Durland, J.E. Jones, J.S. Raleigh, *J. Org. Chem.* 60 (1995) 4146–4152.
- [51] G.T. Baronetti, S.R. de Miguel, O. Scelza, A.A. Castro, *Appl. Catal. A: Gen.* 24 (1986) 109–116.
- [52] D.N. Blakely, G.A. Somorjai, *J. Catal.* 42 (1976) 181–196.
- [53] C.R. Apesteguía, J. Barbier, *Proceedings of the 8th Iberoam. Symp. on Catalysts, Huelva, Spain, 1982*, p. 751.
- [54] H. Lieske, J. Völter, *J. Catal.* 90 (1984) 96–105.
- [55] B.A. Sexton, A.E. Hughes, K. Fogar, *J. Catal.* 88 (1984) 466–477.
- [56] C.D. Wagner, W.M. Riggs, L.E. Davis, J.F. Moulder, G.E. Muilenberg, *Handbook of X-ray Photoelectron Spectroscopy*, Perkin-Elmer Co., Physical Electronics, 1979.
- [57] A.D. Ballarini, P.D. Zgolicz, I.M.J. Vilella, S.R. de Miguel, A.A. Castro, O.A. Scelza, *Appl. Catal. A: Gen.* 381 (2010) 83–91.
- [58] N. Homs, J. Llorca, M. Riera, J. Jolis, J. Fierro, J. Sales, P. Ramírez de la Piscina, *J. Mol. Catal. A: Gen.* 200 (2003) 251–259.
- [59] J. Llorca, P. Ramírez de la Piscina, J. Fierro, J. Sales, N. Homs, *J. Mol. Catal. A: Gen.* 118 (1997) 101–111.
- [60] C.L. Lau, G.K. Wertheim, *J. Vac. Sci. Technol.* 15 (1978) 622–624.
- [61] F. Delbecq, P. Sautet, *J. Catal.* 211 (2002) 398–406.
- [62] F. Delbecq, P. Sautet, *J. Catal.* 152 (1995) 217–236.